

Revisiting Deepfake Detection: Chronological Continual Learning and the Limits of Generalization

Federico Fontana
Sapienza University of Rome
federico.fontana@uniroma1.it

Anxhelo Diko
Sapienza University of Rome
anxhelo.diko@uniroma1.it

Romeo Lanzino
Sapienza University of Rome
romeo.lanzino@uniroma1.it

Marco Raoul Marini
Sapienza University of Rome
marco.marini@uniroma1.it

Bachir Kaddar
University Ibn Khaldoun of Tiaret
b.kaddar@univ-tiaret.dz

Gian Luca Foresti
University of Udine
gianluca.foresti@uniud.it

Luigi Cinque
Sapienza University of Rome
luigi.cinque@uniroma1.it

Abstract

The rapid evolution of deepfake generation technologies poses critical challenges for detection systems, as non-continual learning methods demand frequent and expensive retraining. We reframe deepfake detection (DFD) as a Continual Learning (CL) problem, proposing an efficient framework that incrementally adapts to emerging visual manipulation techniques while retaining knowledge of past generators. Our framework, unlike prior approaches that rely on unreal simulation sequences, simulates the real-world chronological evolution of deepfake technologies in extended periods across 7 years. Simultaneously, our framework builds upon lightweight visual backbones to allow for the real-time performance of DFD systems. Additionally, we contribute two novel metrics: Continual AUC (C-AUC) for historical performance and Forward Transfer AUC (FWT-AUC) for future generalization. Through extensive experimentation (over 600 simulations), we empirically demonstrate that while efficient adaptation (+155 times faster than full retraining) and robust retention of historical knowledge is possible, the generalization of current approaches to future generators without additional training remains near-random (FWT-AUC ≈ 0.5) due to the unique imprint characterizing each existing generator. Such observations are the foundation of our newly proposed Non-Universal Deepfake Distribution Hypothesis. **Code will be released upon acceptance.**

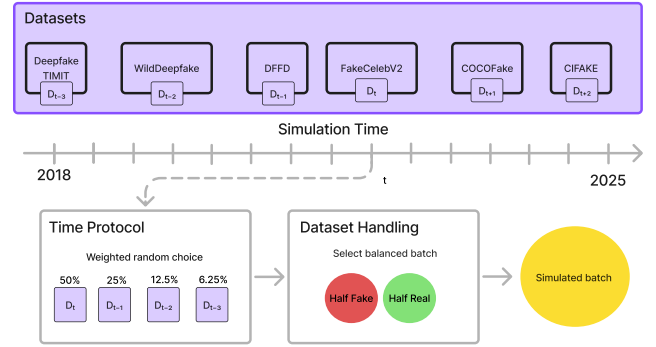


Figure 1. Illustration of the simulation framework spanning from 2018 to 2025. Given a time t , a dataset is selected according to a Time protocol followed by a custom batch extraction which simulates a real-world data stream scenario at the specified time t .

1. Introduction

The evolution of deepfake technology has profound implications for the authenticity of digital media. With novel deepfake generators emerging continuously, traditional deepfake detection (DFD) methods—which rely on static training paradigms—struggle to keep pace. This leads not only to significant computational overhead but also to reduced effectiveness in dynamic, real-world environments. Such challenges are especially critical on social media, where the rapid spread of manipulated content can exacerbate misinformation. Prior works [26, 29, 53] have explored the application of continual learning (CL) for DFD. [29] introduces a continual learning benchmark for DFD with three evaluation sequences based on difficulty or length, applying CL methods in class-incremental (CIL) and domain-

incremental (DIL) settings. [53] builds on this by adding a new generator and evaluating two CL methods, while [26] reframes DFD as a CIL, focusing on DFD generalization.

However, current approaches prove useful only in a small number of CL methods [53], utilize a very limited evaluation set [26] ($\leq 2K$ samples), or employ a not chronological sequence of deepfake generators [26, 29, 53]. To our knowledge, no prior work addresses the DFD as a real-world scenario; rather, the sequence of generators fed to the CL methods is chosen either randomly, based on generator affinity, or according to the difficulty detectors face in recognizing them. As a result, existing research cannot be directly related to real-world settings, as the experimental assumptions for training and evaluation do not reflect real conditions. Furthermore, no in-depth study on data efficiency has been conducted for CL methods, nor has a study on training and inference efficiency been made. Without efficient training and inference, detection models risk becoming obsolete and unable to keep pace with the continuous advancements. Optimizing efficiency ensures maintainability, making DFD systems viable for deployment in high-stakes environments such as social media monitoring.

Motivated by these works, we propose a pipeline that chronologically simulates a deepfake scenario over extended periods using datasets ordered by time, along with a strategy to simulate the sequence of tasks as a random sample from a datastream in any moment (e.g., social media) as illustrated in Fig. 1. This design aims to better capture a real-world deepfake scenario for training and evaluation while avoiding the choice bias on the generator sequence. Additionally, we frame the problem as a DIL task to maintain a detector with consistent size, speed, and memory usage throughout its lifetime. Our focus also extends to the need for data, training, and inference efficiency. Therefore, the proposed method employs lightweight models that can achieve real-time performance on most smartphones and requires significantly lower data to be trained due to the CL strategies, while maintaining competitive performance.

We conducted a total of over 600 full simulations on the presented chronological framework and observed a striking pattern: while some methods successfully retained knowledge of past deepfake generators, none exhibited strong generalization to future ones. To systematically capture this phenomenon, we introduce two new evaluation metrics to measure the retention of past knowledge in highly imbalanced classes and one to quantify a model’s generalizability to chronologically unseen deepfake generators on unbalanced classes. Our analysis using these metrics revealed a fundamental decorrelation between past and future generalization, challenging the assumption that deepfake detection models can generalize across time. This leads us to formally propose the Non-Universal Deepfake Distribution Hypothesis, which states that deepfake detection cannot be

effectively generalized through static training because each deepfake generator imprints a unique, non-transferable signature. We empirically validate this hypothesis.

In summary, our main contributions are:

- We propose a novel **Chronological CL framework** for DFD that mirrors real-world deepfake evolution.
- We evaluated **8 different CL strategies and 4 models** within the proposed framework, demonstrating adaptation while efficiently preserving historical knowledge.
- We introduce **Continual AUC (C-AUC)** and **Forward Transfer AUC (FWT-AUC)** metrics to measure the stability and transferability of the learned detection capabilities in a chronological and unbalanced classes setting.
- We propose the *Non-Universal Deepfake Distribution Hypothesis*, suggesting that each deepfake generator leaves a unique, non-transferable signature, requiring continuous model updates. We support this hypothesis with empirical evaluation on more than 600 simulations.

2. Related Work

2.1. Continual Learning

CL tackles the challenge of catastrophic forgetting [15], where models lose previously acquired knowledge when sequentially trained on new tasks. In DIL[56], tasks share the same label space but differ in input distributions, and task identities are not provided during training or testing. A naive sequential training method, lacking any CL mechanism, serves as a baseline for comparison. More advanced approaches include the Replay strategy [48], which retains and replays stored samples, and Elastic Weight Consolidation (EWC) [24], a regularization method that penalizes significant alterations to the weights critical for past tasks. Based on these, Class-Semantic Replay (CLS-ER) [3] leverages semantic information to focus memory retention on task-relevant features, while Error-Sensitive Memory Replay (ESMER) [52] dynamically adjusts the contribution of stored samples based on their error sensitivity. Additionally, Dark Experience Replay++ (DER++) [5] incorporates knowledge distillation to transfer useful information between tasks, improving performance in CL scenarios.

2.2. Deepfake Detection

Recent advances in deepfake detection have shifted from exploiting low-level artifacts—such as unnatural blinking [30] and inconsistent physiological signals [8]—to focusing on facial warping [31], head pose anomalies [66], and textural irregularities [17]. CNN architectures, notably XceptionNet [50] enhanced with attention [41], have significantly improved artifact detection. To alleviate data scarcity and adapt to evolving deepfakes, self-supervised [19] and semi-supervised methods [9] have been proposed.

The emergence of diffusion models [49] has introduced

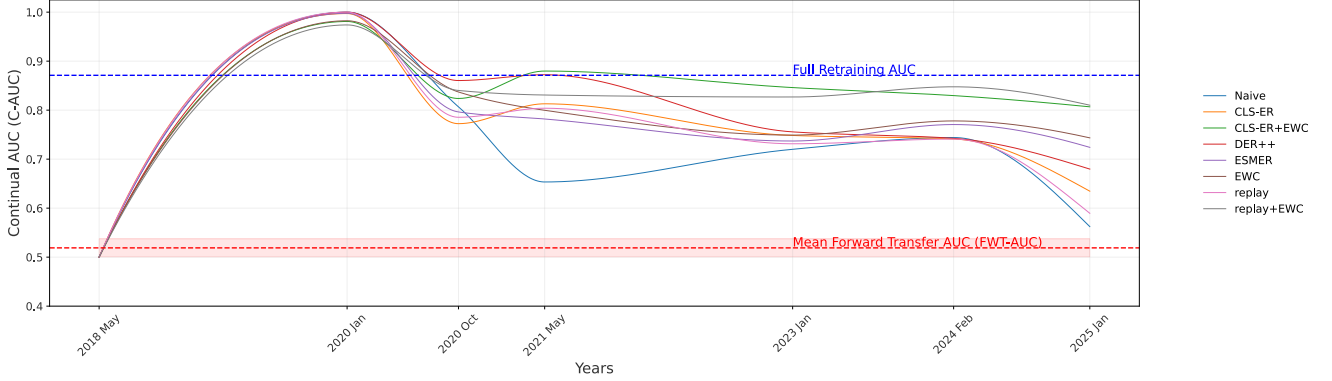


Figure 2. The lines represent the 8 CL methods evaluated on MobileNetV4, each configured with its optimal hyperparameters found in the ablation study. The C-AUC (Eq. 5) indicates the classifiers’ performance on the test data available up to that point. The red horizontal line represents the mean FWT-AUC (Eq. 6) across all experiments, reflecting the methods’ generalization performance on unseen datasets, with the red bars indicating the standard deviation. The blue horizontal line denotes the Eval AUC achieved by the full-retraining method.

new challenges, as these methods often lack the grid-like artifacts typical of GANs [42, 46, 51]. Investigations into intrinsic local dimensionality [37] and reconstruction errors [58] have been undertaken, while advanced architectures such as CNNs and Transformers [2] further push detection limits. Deep learning-based approaches [6, 7, 12–14, 18, 20, 21, 32, 33, 35, 38, 44, 58, 63, 65, 68–70] have achieved notable performance gains despite persistent fairness issues [39, 40, 54, 59, 61]. Recent efforts address these challenges by disentangling demographic and forgery features [34], refining optimization strategies [22], reexamining up-sampling effects, and augmenting latent spaces [62]. Efficiency for real-time deployment is also underscored [27]. Some studies have aimed to understand and improve deepfake generalization. For instance, [67] re-frames the generalization problem from a game-theoretical perspective, [28] examines the zero-shot performance of detectors and the contribution of individual neurons to generalization, and [64] investigates how video blending influences the generalization of video deepfake detectors.

A promising trend is integrating CL into DFD systems. [55] presents an approach that improves robustness by updating the model incrementally without needing full retraining. Specifically, [29] introduces a CL benchmark for DFD that presents three evaluation sequences based on difficulty or length and applies various CL methods in CIL and DIL settings. Building on this, [53] enhances the benchmark by incorporating a new generator and evaluates two CL methods on it, while [26] reframes deepfake detection in a CIL setup, focusing on generalization. Despite advances in CL for DFD, key challenges remain. Notably, current methods ignore the chronological nature of real-world deployment, use limited datasets, and overlook practical constraints like computational efficiency. Contrarily, our approach simulates deepfake evolution over extended periods,

enabling realistic evaluation of model adaptability, retention, and generalization for effective detection while preserving efficiency and real-time inference.

3. Method

3.1. Problem Formulation

Traditional binary DFD systems assume simultaneous access to a complete dataset D composed of samples from a set of deepfake generators $\mathcal{G} = \{g_1, g_2, \dots, g_n\}$. The classifier C is trained by minimizing the empirical risk:

$$\min_C \frac{1}{|D|} \sum_{(x,y) \in D} \ell(C(x), y) \quad (1)$$

where each (x, y) represents an input-label pair (with labels 0 for real and 1 for fake) and ℓ is a suitable loss function, such as cross-entropy. When a new deepfake generator g_{n+1} emerges, the updated dataset becomes $D' = D \cup D_{n+1}$, requiring a complete retraining of C . This approach is computationally expensive and inefficient, especially as the number of generators increases.

To alleviate this problem, as previous works [43], we reformulate the problem within a DIL framework. In this setting, the classifier is updated sequentially: At time step t , the classifier C_t is trained only on the current dataset D_t generated by g_t , while still maintaining performance in all domains previously encountered. Specifically, t represents different stages of the simulation; each time step corresponds to a time span that can be adjusted as a hyperparameter. The optimization objective is given by:

$$\min_{C_t} L(C_t, D_t) + \lambda \Omega(C_t, C_{t-1}) \quad (2)$$

where $L(C_t, D_t)$ is the classification loss on the current domain, $\Omega(C_t, C_{t-1})$ is a regularization term that enforces the

retention of previously learned knowledge (thereby mitigating catastrophic forgetting), and λ is a hyperparameter that balances the trade-off between learning new information and preserving past information. In our work, we further impose a chronological constraint on the DIL framework. That is, the sequence of deepfake generators—and consequently their corresponding datasets—are released and processed in their natural temporal order. Reordering based on similarity, or any reordering in general, is not allowed. Each dataset D_t is observed strictly in the order $t = 1, 2, \dots, T$, reflecting the evolving nature of deepfake generation techniques over time. Although the underlying formulation remains identical to standard DIL, this chronological constraint ensures that the classifier’s adaptation is aligned with real-world scenarios where new generators are introduced sequentially.

3.2. Binary Deepfake Detection under Chronologically Domain Incremental Learning

In our approach, we enforce a strict temporal ordering of data acquisition that mirrors the natural release of deepfake generators. Specifically, the model is updated sequentially following the authentic timeline without any reordering or artificial sampling of past data. At each chosen interval, new balanced batches are integrated into the learning process according to timeline protocol (see Sec. 3.2.1). The temporal distribution and key attributes of the datasets are summarized in Table 1.

3.2.1. Timeline Protocol

The timeline protocol simulates the natural evolution of deepfake generation by associating each dataset D_1, D_2, \dots, D_N with its unique release date t_i (where $t_1 < t_2 < \dots < t_N$). At each update interval, as illustrated in Fig. 1, the selection of datasets is governed by an exponentially weighted random selection model, which mirrors the historical distribution of deepfake instances. Specifically, the probability of selecting dataset D_i is defined as:

$$P(D_i) = \frac{0.5 \cdot (0.5^i)}{\sum_{j=0}^{N-1} 0.5 \cdot (0.5^j)} \quad (3)$$

with the normalization condition:

$$\sum_{i=0}^{N-1} P(D_i) = 1 \quad (4)$$

Datasets are sampled in reverse chronological order relative to the current simulation time, thereby prioritizing more recent data. A crucial aspect of this simulation is its attempt to replicate the actual distribution of deepfake samples as observed at a given historical moment. In practice, at any specific point in time, adapting the model to new tasks would

require sampling random deepfake instances from contemporary sources, such as social networks. This approach mirrors real-world deployment scenarios where a model is continuously updated to detect emerging deepfake techniques by leveraging naturally occurring data streams.

3.3. Evaluation Metrics

To quantify performance in the presented environment, we propose two metrics: *Continual AUC (C-AUC)* and *Forward Transfer AUC (FWT-AUC)*. These extend established CL concepts to address the unique challenges of DFD, where datasets are typically highly imbalanced. Conventional metrics, like accuracy, are often inadequate for such tasks as they assume a balanced class distribution, which does not reflect the nature of most real-world DFD datasets. The evolving generation techniques and significant class imbalance in deep fake datasets demand robustness beyond traditional accuracy metrics.

3.3.1. Continual AUC

C-AUC measures retention on previously encountered data:

$$\text{C-AUC}(t) = \frac{1}{|D_{1:t}|} \sum_{i=1}^{|D_{1:t}|} [\text{AUC}(C_t, D_i)] \quad (5)$$

where $D_{1:t}$ are the datasets presented up to time t and C_t is the detector at t . This metric is related to *Average Accuracy* and *Backward Transfer* [36] but uses Area Under The Curve (AUC) instead of accuracy, better-capturing robustness to class imbalance. Measures **stability**[16], which refers to retention of knowledge in previous and current tasks.

3.3.2. Forward Transfer AUC

FWT-AUC quantifies generalization to future generators:

$$\text{FWT-AUC}(t) = \frac{1}{|D_{t+1:}|} \sum_{i=1}^{|D_{t+1:}|} [\text{AUC}(C_t, D_i)] \quad (6)$$

where $D_{t+1:}$ are the dataset not yet released a time t . This metric aligns with *Forward Transfer (FWT)* [36] but uses AUC to evaluate generalization to future tasks.

4. Experiments

In the first part of this section, we clarify the choice of models and the CL strategies that were tested, and then we present the results.

4.1. Models

To balance efficiency in both training and inference, we employ a subset of lightweight models, specifically: FastViT-T8 [57], ConvNeXtV2-ATTO [60], ViT-Tiny [11], and MobileNetV4-Medium [45]. The size of these models was chosen based on the GPU time required for single-task

Dataset	Type	Resolution	Data Count	Sources	Month	Year
DeepfakeTIMIT [25]	Video	128 × 128	620 videos	Faceswap-GAN (based on VidTIMIT)	July	2018
WildDeepfake [71]	Video	Variable	7,314 face sequences (from 707 videos)	Internet	October	2020
DFFD [10]	Image	Variable	Heterogeneous content	FFHQ, CelebA, FF++	N/A	2020
FakeAVCelebv2 [23]	Video	Variable	20,000 face sequences	Faceswap, FSGAN	N/A	2021
COCOFake [1]	Image	Variable	1,200,000 images	Stable Diffusion v1.4, v2.0	N/A	2023
CIFAKE [4]	Image	Variable	120,000 images (60k real + 60k synthetic)	Stable Diffusion v1.4	February	2024

Table 1. Datasets used for the CL setup, including resolution, data count, sources, release month, and publication year.

Strategy	Model	Monthly Batches = 10			Monthly Batches = 20			Monthly Batches = 50		
		AUC	Mean C-AUC	Mean FWT-AUC	AUC	Mean C-AUC	Mean FWT-AUC	AUC	Mean C-AUC	Mean FWT-AUC
Full Retraining		0.871	-	-	0.8711	-	-	0.871	-	-
CLS-ER+EWC	MobileNetV4-M [45]	0.765	0.803	0.520	0.793	0.801	0.545	0.852	0.857	0.482
Replay+EWC		0.745	0.792	0.527	0.760	0.822	0.469	0.841	0.840	0.504
EWC [24]		0.733	0.784	0.475	0.743	0.815	0.503	0.806	0.753	0.499
ESMER[52]		0.727	0.739	0.519	0.759	0.776	0.573	0.741	0.664	0.528
DER++[5]		0.720	0.798	0.547	0.662	0.785	0.554	0.746	0.778	0.518
Replay[48]		0.681	0.758	0.509	0.711	0.691	0.528	0.740	0.752	0.521
CLS-ER [3]		0.640	0.746	0.493	0.635	0.784	0.523	0.703	0.569	0.492
Naive		0.607	0.742	0.518	0.567	0.712	0.520	0.593	0.702	0.515
Full Retraining		0.960	-	-	0.960	-	-	0.960	-	-
CLS-ER+EWC	ViT-Tiny [11]	0.673	0.718	0.556	0.768	0.818	0.507	0.796	0.807	0.518
Replay+EWC		0.679	0.699	0.552	0.799	0.779	0.537	0.818	0.824	0.512
EWC [24]		0.663	0.702	0.498	0.781	0.764	0.516	0.808	0.808	0.520
ESMER[52]		0.556	0.667	0.510	0.839	0.813	0.490	0.783	0.857	0.504
DER++[5]		0.704	0.724	0.47	0.826	0.789	0.504	0.808	0.811	0.517
Replay[48]		0.637	0.709	0.563	0.790	0.777	0.515	0.798	0.813	0.530
CLS-ER [3]		0.700	0.763	0.507	0.793	0.824	0.496	0.932	0.915	0.528
Naive		0.662	0.700	0.506	0.616	0.683	0.476	0.777	0.798	0.512
Full Retraining		0.861	-	-	0.861	-	-	0.861	-	-
CLS-ER+EWC	ConvNeXtV2-ATTO [60]	0.719	0.804	0.502	0.706	0.785	0.539	0.681	0.722	0.527
Replay+EWC		0.638	0.700	0.537	0.748	0.776	0.545	0.758	0.776	0.526
EWC [24]		0.664	0.722	0.535	0.705	0.746	0.530	0.744	0.751	0.540
ESMER[52]		0.631	0.713	0.522	0.548	0.704	0.554	0.811	0.821	0.505
DER++[5]		0.689	0.742	0.532	0.728	0.764	0.551	0.764	0.783	0.539
Replay[48]		0.678	0.706	0.540	0.753	0.777	0.545	0.766	0.770	0.519
CLS-ER [3]		0.706	0.746	0.547	0.748	0.767	0.530	0.827	0.857	0.499
Naive		0.664	0.722	0.535	0.492	0.637	0.473	0.636	0.720	0.541
Full Retraining		0.726	-	-	0.726	-	-	0.726	-	-
CLS-ER+EWC	FastViT-T8 [57]	0.686	0.651	0.502	0.584	0.642	0.530	0.587	0.613	0.491
Replay+EWC		0.468	0.699	0.518	0.452	0.663	0.503	0.636	0.643	0.502
EWC [24]		0.568	0.669	0.506	0.637	0.632	0.505	0.477	0.704	0.520
ESMER[52]		0.634	0.651	0.527	0.663	0.689	0.571	0.624	0.611	0.511
DER++[5]		0.573	0.666	0.527	0.600	0.659	0.557	0.573	0.556	0.542
Replay[48]		0.593	0.555	0.527	0.628	0.631	0.559	0.558	0.752	0.513
CLS-ER [3]		0.478	0.671	0.551	0.459	0.669	0.528	0.705	0.730	0.536
Naive		0.529	0.647	0.543	0.452	0.459	0.509	0.502	0.696	0.530

Table 2. Evaluation of strategies across different monthly batches on the evaluation set of the datasets for four different models.

training, ensuring a balance between efficiency and performance. We set the input size to 384x384. Our method utilizes a single, compact model that relies solely on visual data, excluding the vocal aspects of deepfakes. Each video sample consists of five consecutive frames, allowing the model to effectively capture temporal patterns and visual cues. The frames are processed individually, and the final class prediction is obtained by averaging the highest probabilities across frames.

4.2. Continual learning Strategies

A diverse set of CL strategies was used. The **Naive** approach follows a simple sequential training paradigm without integrating any continual learning mechanisms. In contrast, **Replay** [48] mitigates forgetting by storing and reusing samples from previous tasks. Regularization-based techniques such as **EWC** [24] (Elastic Weight Consolidation) impose penalties on changes to parameters identified as crucial for past tasks. Extending replay methods, **CLS-ER** [3] (Class-Semantic Replay) refines memory replay by incorporating class-semantic information,

Method	Model	Monthly Batches = 10			Monthly Batches = 20			Monthly Batches = 50		
		Monthly GPU Time (s)	Total GPU Time (min)	Unique Samples	Monthly GPU Time (s)	Total GPU Time (min)	Unique Samples	Monthly GPU Time (s)	Total GPU Time (min)	Unique Samples
Full Retraining		-	3130.02 * \mathcal{N}	5773248	-	3130.02 * \mathcal{N}	5773248	-	3130.02 * \mathcal{N}	5773248
CLS-ER+EWC Replay+EWC EWC [24] ESMER[52] DER++[5] Replay [48] CLS-ER [3] Naive	MobileNetV4-M [45]	3.5	4.67	12800	4.73	6.31	25600	13.76	18.35	64000
		3.11	4.15		4.25	5.67		10.09	13.45	
		0.91	1.21		1.75	2.33		4.35	5.80	
		2.25	3.00		4.66	6.21		11.38	15.17	
		1.69	2.25		3.08	4.11		8.06	10.75	
		2.54	3.39		3.24	4.32		8.04	10.72	
		3.25	4.33		4.47	5.96		12.41	16.55	
		0.9	1.20		0.99	1.32		2.5	3.33	
Full Retraining		-	4451.55 * \mathcal{N}	5773248	-	4451.55 * \mathcal{N}	5773248	-	4451.55 * \mathcal{N}	5773248
CLS-ER+EWC Replay+EWC EWC [24] ESMER[52] DER++[5] Replay [48] CLS-ER [3] Naive	ViT-Tiny [11]	1.52	2.03	12800	2.39	3.19	25600	9.52	12.69	64000
		1.32	1.76		1.16	1.55		2.79	3.73	
		0.48	0.64		0.92	1.23		2.46	3.27	
		1.19	1.59		3.09	4.13		10.26	13.68	
		0.88	1.18		1.18	1.57		3.01	4.01	
		0.49	0.65		0.77	1.02		3.53	4.71	
		0.28	0.38		3.61	4.81		5.11	6.81	
		1.28	1.71		0.53	0.70		1.45	1.93	
Full Retraining		-	930 * \mathcal{N}	5773248	-	930 * \mathcal{N}	5773248	-	930 * \mathcal{N}	5773248
CLS-ER+EWC Replay+EWC EWC [24] ESMER[52] DER++[5] Replay [48] CLS-ER [3] Naive	ConvNeXtV2-ATTO [60]	1.53	2.04	12800	2.37	3.17	25600	5.72	7.63	64000
		0.64	0.85		1.14	1.53		2.58	3.44	
		0.47	0.63		0.76	1.01		2.20	2.94	
		1.76	2.35		2.41	3.22		7.53	10.04	
		0.97	1.29		1.33	1.77		3.37	4.50	
		0.49	0.66		0.72	0.96		1.89	2.52	
		1.42	1.89		2.09	2.79		5.12	6.83	
		0.27	0.36		0.50	0.66		1.39	1.85	
Full Retraining		-	1.669.33 * \mathcal{N}	5773248	-	1.669.33 * \mathcal{N}	5773248	-	1.669.33 * \mathcal{N}	5773248
CLS-ER+EWC Replay+EWC EWC [24] ESMER[52] DER++[5] Replay [48] CLS-ER [3] Naive	FastViT-T8 [57]	2.59	3.46	12800	4.27	5.70	25600	9.91	13.22	64000
		2.33	3.11		1.92	2.56		4.68	6.24	
		0.83	1.10		1.41	1.89		4.01	5.35	
		3.30	4.40		5.45	7.26		9.55	12.74	
		1.72	2.30		1.94	2.58		4.94	6.59	
		0.96	1.28		1.30	1.74		3.01	4.02	
		2.22	2.97		3.87	5.17		8.57	11.43	
		0.47	0.63		0.77	1.03		2.59	3.45	

Table 3. Comparison of GPU time and unique samples seen across different monthly batches. "Monthly GPU Time (s)" represents the monthly processing time in seconds, "Total GPU Time (min)" indicates the total GPU time in minutes over the entire simulation, and "Unique Samples" refers to the number of distinct samples encountered. The Full Retraining remains independent of monthly batches. The variable \mathcal{N} denotes the number of adaptations training, where $\mathcal{N} = 1$ represents a single training session, $\mathcal{N} = 2$ indicates one retraining iteration, and so on, ensuring adaptation to newly emerging generators.

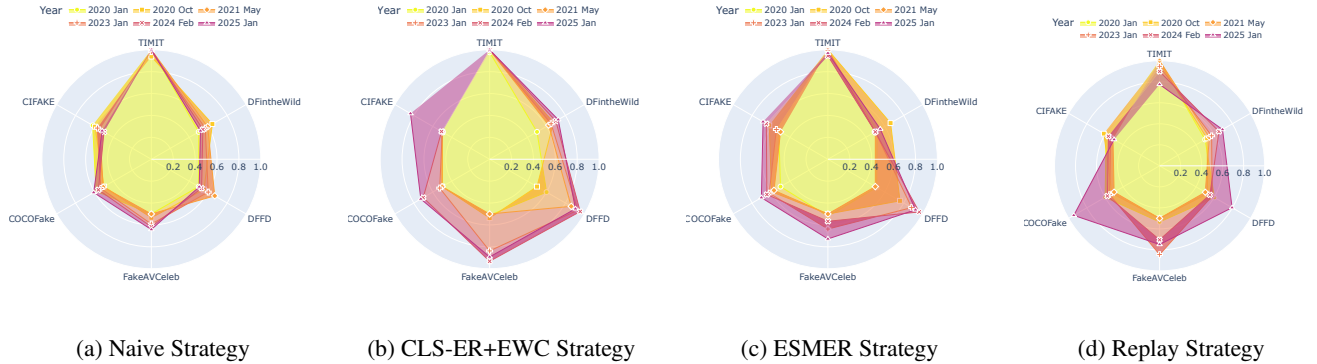


Figure 3. Spider charts showing the evaluation AUC on each dataset for each evaluation step using different strategies.

while **CLS-ER+EWC** combines replay with regularization for improved retention. A more adaptive replay mechanism, **ESMER** [52] (Error-Sensitive Memory Replay), adjusts sample contributions according to their error sensitivity. Furthermore, **DER++** [5] (Dark Experience Replay++) enhances replay strategies through knowledge distillation. Lastly, a hybrid approach, **Replay+EWC**, synergistically integrates the strengths of both Replay and EWC. Each of these methods presents distinct advantages and trade-offs in combating catastrophic forgetting, and their comparative evaluation investigates effective CL methodologies.

4.3. Full Retraining Baselines

To establish a baseline model that serves as a reference for all continual learning strategies, we fine-tuned the models

pre-trained on ImageNet21K [47] using the datasets presented in Tab. 1. The training was performed using the AdamW optimizer with a learning rate of 10^{-6} and employed a Cosine Annealing Learning Rate Scheduler with $T_{\max} = 100,000$ iterations. Each batch comprised 16 samples per dataset (resulting in a total batch size of 96 samples) with a balanced composition of 8 real and 8 fake samples per subset, and training was carried out for 100,000 iterations. The baseline models were subsequently evaluated on the test sections of the six datasets mentioned above.

4.4. Experimental Setup

All experiments were conducted on a 14th-generation Intel i9 processor and an NVIDIA RTX 4090 GPU. We evaluate each CL method within the presented framework. The

tasks are introduced on a monthly basis. For every newly released dataset, a complete model evaluation is performed, including the AUC, C-AUC, FWT-AUC, and GPU time. The experiments are categorized into three groups based on the number of monthly tasks: 10, 20, and 50. For each scenario, the models are trained with the corresponding number of batches per simulated month. Consequently, during the simulation, each method processes a total of $80 \times \text{monthly batches} \times 16$ samples, where 16 represents the batch size. AdamW is used as the optimizer for all experiments. For the ESMER method, we set the parameters as follows: $\beta = 1$, $\alpha = 0.9$, and the update decay for the stable model weight is set to 0.99. For EWC and Replay+EWC, the stable model weight update decay is set to 0.99. The CLS-ER and CLS-ER+EWC use a plastic model update decay of 0.99 and a stable model update decay of 0.999. When the monthly batch size is 50, the learning rate for the Naive, Replay, CLS-ER+EWC, Replay+EWC, EWC, and DER++ versions is set to 1×10^{-5} , while for ESMER and CLS-ER, the learning rate is set to 1×10^{-4} . The memory buffer size is set to 50 for all techniques except for Replay, which has a memory buffer size of 10. Additionally, for Replay, Replay+EWC, and CLS-ER, the regularization coefficient λ is set to 10. For ESMER and CLS-ER+EWC, $\lambda = 0.5$, and for EWC, $\lambda = 0.1$. When the monthly batch size is 20, the learning rate for Naive is set to 1×10^{-3} , and for Replay, CLS-ER+EWC, Replay+EWC, EWC, and DER++, the learning rate is 1×10^{-5} . For CLS-ER and ESMER, the learning rate is set to 1×10^{-4} . The memory buffer size is 100 for CLS-ER+EWC, ESMER, and CLS-ER, and 50 for the other techniques. For Replay+EWC, CLS-ER+EWC, and CLS-ER, the regularization coefficient λ is set to 10. For Replay, λ is set to 1, and for DER++, λ is set to 0.5. When the monthly batch size is 10, the learning rate for Naive, DER++, and EWC is set to 1×10^{-5} , while for CLS-ER+EWC, Replay+EWC, ESMER, Replay, and CLS-ER, the learning rate is set to 1×10^{-4} . The memory buffer size is 100 for CLS-ER+EWC, Replay+EWC, ESMER, DER++, Replay, and CLS-ER.

4.5. Results

Performance of CL Strategies: Tab. 2 compares the performance of CL strategies with the complete baseline of retraining. The results indicate that all CL approaches outperform the naive method. Moreover, in the largest monthly batch setting, the methods match the rooftops closely. CLS-ER+EWC and Replay+EWC, which incorporate both replay and semantic memory mechanisms, perform well in the monthly batch 10 configuration. However, in the monthly batch 20 and 50 setups, each model favors a specific approach, suggesting that each method would benefit from its own dedicated hyperparameter tuning. The best overall performance is achieved with ViT-T in

the monthly batch 50 setup, reaching an AUC of 0.932 and a Mean C-AUC of 0.915. FastViT exhibits the lowest performance. Overall, increasing monthly batches improves C-AUC, highlighting the importance of sufficient data for stability. In contrast, regularization-only methods like EWC show limited scalability. **Generalization Limitations:** All strategies exhibit near-random FWT-AUC (0.49 – 0.57), regardless of monthly batch configuration, method or model. Even ViT-T with CLS-ER, the best-performing strategy is random guessing, confirming that each generator introduces unique artifacts. **Computational Efficiency:** Tab. 3 reveals a clear efficiency hierarchy. Naive fine-tuning requires minimal overhead (0.27-2.59 min total GPU time), while combined replay-regularization methods (CLS-ER+EWC) demand 0.64-18.35 min. Despite this overhead, all continual methods remain orders of magnitude more efficient than full retraining (155 times less GPU Time). The chosen architectures enable real-time inference, making even intensive strategies viable on mobile devices. **Tradeoffs Between Stability and Generalization:** While C-AUC improves with an increased number of monthly batches, FWT-AUC remains relatively stagnant. For instance, Replay+EWC on MobileNetV4 boosts C-AUC by 7.8% (from 0.792 to 0.840) when scaling from 10 to 50 batches, yet its FWT-AUC only fluctuates between 0.469 and 0.504. This suggests that stability, as measured by C-AUC, is influenced by the replay buffer size, the regularization strength, method and model, whereas generalization, indicated by FWT-AUC, is fundamentally constrained by distribution shifts between generators. The absence of a correlation between C-AUC and FWT-AUC confirms that these objectives are distinct. Although replay mechanisms help mitigate forgetting, they do not facilitate transfer learning across non-stationary generator distributions.

4.6. The Non-Universal Deepfake Distribution Hypothesis

In all the conducted experiments, despite extensive hyperparameter tuning, different methods and models, the *FWT-AUC* consistently remains close to 0.5. This result indicates the classifier behaves randomly on future generators. This suggests that each generator leaves a unique signature, and no "distribution of deepfakes" can be generalized. Moreover, this highlights that we cannot rely on a "natural distribution" of deep-fake media. Not all edited images or videos qualify as deepfakes, as naive modifications—such as simple color adjustments, font changes, or montages—do not constitute deepfake manipulations. The *Non-Universal Deepfake Distribution Hypothesis* seeks to capture the temporal evolution of a detector’s effectiveness as the underlying deepfake generators evolve over time. The hypothesis highlights the need for CL that can respond to the rapid evolution of deepfake generators,

ensuring sustained robustness in real-world applications.

Hypothesis Statement: Deepfake detection cannot be generalized through static training.

4.6.1. Formulation

Let \mathcal{G} denote the space of deepfake generators evolving through discrete time steps. For any temporal window $T = [1, N] \subseteq \mathbb{N}$ with $t \in T$, let $C_{1:t}^s$ represent a classifier trained on synthetic images of generators $G_{1:t}$ using the strategy $s \in \mathcal{S}$, where \mathcal{S} is the set of training methodology and hyperparameter configuration. Let $\mathcal{D}(G)$ be the function that returns a dataset comprising real and fake images, given a generator or a set of generators. **Transferability Semantics:** The *maximum temporal transferability* quantifies the classifier’s ability to generalize from past data to the next generator:

$$\mathcal{T}_{\max} = \max_{t \in T, s \in \mathcal{S}} \left(\underbrace{\text{AUC}(C_{1:t}^s, \mathcal{D}(G_{t+1}))}_{\text{Future generalization}} - 0.5 \right) \quad (7)$$

Note: We subtract 0.5 because an AUC of 0.5 corresponds to the performance of random guessing in binary classification. This normalization centers the metric at zero, making it easier to interpret.

Decay Dynamics: The *transfer decay factor* quantifies progressive performance erosion:

$$\mathcal{T}_{\text{decay}} = \mathbb{E}_{s \in \mathcal{S}, t \in T} \left[\frac{\text{AUC}(C_{1:t}^s, \mathcal{D}(G_{t+2})) - 0.5}{\text{AUC}(C_{1:t}^s, \mathcal{D}(G_{t+1})) - 0.5} \right] \quad (8)$$

In the case $\mathcal{T}_{\text{decay}} < 1$ it leads to a compounded degradation model for k -step generalization even for the best strategy:

$$\mathcal{T}_{\text{comp}} = 0.5 + \mathcal{T}_{\max} \cdot (\mathcal{T}_{\text{decay}})^k \quad (9)$$

Empirical Parameterization: Under experimental conditions, the temporal window $T \approx \bar{T} = [1, 6]$ aligns with the dataset release chronology presented in the method. The strategy space $\mathcal{S} \approx \bar{\mathcal{S}}$ includes all CL methods used in the methods section and all hyperparameter configurations in the ablation study, with $|\bar{\mathcal{S}}| = 618$. Additionally, $\mathcal{D}(G_k) \approx D_k$ represents the test set of the k -th dataset.

Using this setup we derive:

$$\mathcal{T}_{\max} \approx \overline{\mathcal{T}_{\max}} = \max_{t \in \bar{T}, s \in \bar{\mathcal{S}}} \left(\underbrace{\text{AUC}(C_{1:t}^s, D_{t+1})}_{\text{Future generalization}} - 0.5 \right) \quad (10)$$

The value $\overline{\mathcal{T}_{\max}} = 0.094$ is observed across all CL strategies and hyperparameters, highlighting fundamental limitations in the classifier trained on historical data and evaluated

on data generated on the next generators.

$$\mathcal{T}_{\text{decay}} \approx \overline{\mathcal{T}_{\text{decay}}} = \frac{1}{|\bar{\mathcal{S}}||\bar{T}|} \sum_{s \in \bar{\mathcal{S}}} \sum_{t \in \bar{T}} \frac{\text{AUC}(C_{1:t}^s, D_{t+2}) - 0.5}{\text{AUC}(C_{1:t}^s, D_{t+1}) - 0.5} \quad (11)$$

The empirical value $\overline{\mathcal{T}_{\text{decay}}} = 0.54$, calculated across all CL strategies and hyperparameters (selecting only experiments where the classifier achieved at least 0.75 on evaluation AUC), indicates that residual classification capacity decays exponentially. This leads to a compounding degradation process:

$$\begin{aligned} \mathcal{T}_{\text{comp}} \approx \overline{\mathcal{T}_{\text{comp}}} &= 0.5 + (\overline{\mathcal{T}_{\max}}) \cdot (\overline{\mathcal{T}_{\text{decay}}})^k = \\ &= 0.515 \approx \text{Random guessing} \end{aligned} \quad (12)$$

This empirical characterization suggests that *any static detector* $C_{1:t}^s$ inevitably converges to random guessing against evolving generators G_{t+k} in a very short time in the setup proposed even the best strategy turns to random guessing in 3 time units.

4.7. Ablation Study

In our ablation study conducted on MobileNetV4, we evaluate several critical hyperparameters. We test three different learning rates— 10^{-5} , 10^{-4} , and 10^{-3} —which determine the optimization step size and significantly affect the model’s learning effectiveness without overfitting. The memory buffer size, which dictates the number of batches stored for replay-based strategies, is examined using two values: 50 and 100. Additionally, we assess the impact of the number of monthly batches by testing configurations with 10, 20, and 50 batches. For the methods EWC, Replay+EWC, ESMER, DER++, and CLS-ER+EWC, we explore various regularization strengths, setting λ_{reg} to 0.1, 0.5, 1, and 10, while for DER++ we also evaluate α over the same range. Fig. 3 visualizes evaluation AUC trajectories of MobileNetV4 across datasets and time steps. CLS-ER+EWC (Fig. 3b) maintains stable performance on historical datasets (C-AUC=0.857), while naive fine-tuning (3a) shows severe forgetting (C-AUC=0.702). All strategies exhibit radial symmetry in the spider charts, confirming the almost temporal independence of generator-specific detection performance. The evaluation spider charts for each configuration are provided in the supplementary material.

5. Conclusion

This paper reframes DFD as a DIL problem with a chronological constraint, to simulate real-case scenario, addressing the challenge of adapting to evolving generation technologies while retaining knowledge of past techniques. Our framework, leveraging lightweight architectures and diverse CL strategies, demonstrates that CL enables efficient adaptation (~ 155 times less GPU time) in respect

with full retraining while maintaining performance on previously encountered generators. However, the near-random FWT-AUC ≈ 0.5 across all strategies empirically validates our *Non-Universal Deepfake Distribution Hypothesis*: each generator leaves unique, non-transferable artifacts, rendering generalization to future techniques fundamentally limited, so DFD cannot be generalized through static training.

These findings reveal an exponential decay pattern in the detection capacity, where residual performance deteriorates to random guessing (0.515 AUC) in 3 time steps. This underscores the inadequacy of static training paradigms and establishes the imperative for CL. Our results suggest that detection systems must prioritize two complementary objectives: (1) efficient retention of historical knowledge through replay and regularization mechanisms, and (2) rapid adaptation pipelines to incorporate emerging techniques with minimal effort.

Our framework demonstrates that deepfake detectors can be updated efficiently using a few data, enabling maintenance by independent actors with limited resources. This efficiency democratizes detection ecosystems, allowing researchers, small organizations, and even community collectives to train and update detectors without reliance on centralized infrastructure or massive computational budgets.

References

- [1] Roberto Amoroso, Davide Morelli, Marcella Cornia, Lorenzo Baraldi, Alberto Del Bimbo, and Rita Cucchiara. Parents and children: Distinguishing multimodal deepfakes from natural images. *arXiv preprint arXiv:2304.00500*, 2023. 5
- [2] Roberto Amoroso, Davide Morelli, Marcella Cornia, Lorenzo Baraldi, Alberto Del Bimbo, and Rita Cucchiara. Parents and children: Distinguishing multimodal deepfakes from natural images. *Arxiv Preprint Arxiv:2304.00500*, 2023. 3
- [3] Elahe Arani, Fahad Sarfraz, and Bahram Zonooz. Learning fast, learning slow: A general continual learning method based on complementary learning system. *Arxiv Preprint Arxiv:2201.12604*, 2022. 2, 5, 6
- [4] Jordan J Bird and Ahmad Lotfi. Cifake: Image classification and explainable identification of ai-generated synthetic images. *IEEE Access*, 12:15642–15650, 2024. 5
- [5] Pietro Buzzega, Matteo Boschini, Angelo Porrello, Davide Abati, and Simone Calderara. Dark experience for general continual learning: a strong, simple baseline. *Advances In Neural Information Processing Systems*, 33:15920–15930, 2020. 2, 5, 6
- [6] Hao Chen, Peng Zheng, Xin Wang, Shu Hu, Bin Zhu, Jinrong Hu, Xi Wu, and Siwei Lyu. Harnessing the power of text-image contrastive models for automatic detection of online misinformation. In *Proceedings of the IEEE/CVF Conference on Computer Vision and Pattern Recognition*, pages 923–932, 2023. 3
- [7] Tiewen Chen, Shanmin Yang, Shu Hu, Zhenghan Fang, Ying Fu, Xi Wu, and Xin Wang. Masked conditional diffusion model for enhancing deepfake detection. *Arxiv Preprint Arxiv:2402.00541*, 2024. 3
- [8] Umur Aybars Ciftci, Ilke Demir, and Lijun Yin. Fakecatcher: Detection of synthetic portrait videos using biological signals. *Ieee Transactions On Pattern Analysis And Machine Intelligence*, 2020. 2
- [9] Davide Cozzolino, Justus Thies, Andreas Rössler, Christian Riess, Matthias Nießner, and Luisa Verdoliva. Forensictransfer: Weakly-supervised domain adaptation for forgery detection. *Conference On Computer Vision And Pattern Recognition*, 2018. 2
- [10] Hao Dang, Feng Liu, Joel Stehouwer, Xiaoming Liu, and Anil K Jain. On the detection of digital face manipulation. In *Proceedings of the IEEE/CVF Conference on Computer Vision and Pattern recognition*, pages 5781–5790, 2020. 5
- [11] Alexey Dosovitskiy, Lucas Beyer, Alexander Kolesnikov, Dirk Weissenborn, Xiaohua Zhai, Thomas Unterthiner, Mostafa Dehghani, Matthias Minderer, Georg Heigold, Sylvain Gelly, et al. An image is worth 16x16 words: Transformers for image recognition at scale. *arXiv preprint arXiv:2010.11929*, 2020. 4, 5, 6
- [12] Bing Fan, Zihan Jiang, Shu Hu, and Feng Ding. Attacking identity semantics in deepfakes via deep feature fusion. In *2023 IEEE 6th International Conference on Multimedia Information Processing and Retrieval (MIPR)*, pages 114–119. IEEE, 2023. 3
- [13] Bing Fan, Shu Hu, and Feng Ding. Synthesizing black-box anti-forensics deepfakes with high visual quality. *Iccasp*, 2024.
- [14] Michael Goebel, Lakshmanan Nataraj, Tejaswi Nanjundaswamy, Tajuddin Manhar Mohammed, Shivkumar Chandrasekaran, and BS Manjunath. Detection, attribution and localization of gan generated images. *Arxiv Preprint Arxiv:2007.10466*, 2020. 3
- [15] Ian J Goodfellow, Mehdi Mirza, Da Xiao, Aaron Courville, and Yoshua Bengio. An empirical investigation of catastrophic forgetting in gradient-based neural networks. *Arxiv Preprint Arxiv:1312.6211*, 2013. 2
- [16] Stephen T Grossberg. *Studies of mind and brain: Neural principles of learning, perception, development, cognition, and motor control*. Springer Science & Business Media, 2012. 4
- [17] Luca Guarnera, Oliver Giudice, and Sebastiano Battiato. Deepfake detection by analyzing convolutional traces. In *Conference on Computer Vision and Pattern Recognition Workshops*, pages 666–667, 2020. 2
- [18] Hui Guo, Shu Hu, Xin Wang, Ming-Ching Chang, and Siwei Lyu. Robust attentive deep neural network for detecting gan-generated faces. *Ieee Access*, 10:32574–32583, 2022. 3
- [19] Chih-Chung Hsu, Yi-Xiu Zhuang, and Chia-Yen Lee. Deep fake image detection based on pairwise learning. *Applied Science.*, 10(1):370, 2020. 2
- [20] Jiashang Hu, Shilin Wang, and Xiaoyong Li. Improving the generalization ability of deepfake detection via disentangled representation learning. In *2021 IEEE International Confer-*

- ence on Image Processing (ICIP), pages 3577–3581. IEEE, 2021. 3
- [21] Nils Hulzebosch, Sarah Ibrahim, and Marcel Worring. Detecting cnn-generated facial images in real-world scenarios. In *Proceedings of the IEEE/CVF conference on computer vision and pattern recognition workshops*, pages 642–643, 2020. 3
- [22] et al. Ju. Improving fairness in deepfake detection. In *Proceedings of the IEEE/CVF Winter Conference on Applications of Computer Vision (WACV)*, 2024. Open Access version available on the CVF website. 3
- [23] Hasam Khalid, Shahroz Tariq, Minha Kim, and Simon S. Woo. FakeAVCeleb: A novel audio-video multimodal deepfake dataset. In *Thirty-fifth Conference on Neural Information Processing Systems Datasets and Benchmarks Track (Round 2)*, 2021. 5
- [24] James Kirkpatrick, Razvan Pascanu, Neil Rabinowitz, Joel Veness, Guillaume Desjardins, Andrei A Rusu, Kieran Milan, John Quan, Tiago Ramalho, Agnieszka Grabska-Barwinska, et al. Overcoming catastrophic forgetting in neural networks. *Proceedings Of The National Academy Of Sciences*, 114(13):3521–3526, 2017. 2, 5, 6
- [25] Pavel Korshunov and Sébastien Marcel. Deepfakes: a new threat to face recognition? assessment and detection. *arXiv preprint arXiv:1812.08685*, 2018. 5
- [26] Raj Kumar, Sunil Patel, Minh Lee, and Li Chen. Towards generalized deepfake detection with continual learning on limited new data. In *Proceedings of the IEEE International Conference on Multimedia and Expo (ICME)*, pages 1234–1239, 2024. 1, 2, 3
- [27] Romeo Lanzino, Federico Fontana, Anxhelo Diko, Marco Raoul Marini, and Luigi Cinque. Faster than lies: Real-time deepfake detection using binary neural networks. In *Proceedings of the IEEE/CVF Conference on Computer Vision and Pattern Recognition*, pages 3771–3780, 2024. 3
- [28] Boquan Li, Jun Sun, Christopher M Poskitt, and Xingmei Wang. How generalizable are deepfake image detectors? an empirical study. *Arxiv Preprint Arxiv:2308.04177*, 2023. 3
- [29] Chuqiao Li, Zhiwu Huang, Danda Pani Paudel, Yabin Wang, Mohamad Shahbazi, Xiaopeng Hong, and Luc Van Gool. A continual deepfake detection benchmark: Dataset, methods, and essentials. In *Proceedings of the IEEE/CVF winter conference on applications of computer vision*, pages 1339–1349, 2023. 1, 2, 3
- [30] Yuezun Li, Ming-Ching Chang, and Siwei Lyu. In icu oculi: Exposing ai created fake videos by detecting eye blinking. In *International Workshop on Information Forensics and Security (WIFS)*, pages 1–7. IEEE, 2018. 2
- [31] Yuezun Li, Xin Yang, Pu Sun, Honggang Qi, and Siwei Lyu. Celeb-df: A large-scale challenging dataset for deepfake forensics. In *Conference on Computer Vision and Pattern Recognition*, pages 3207–3216, 2020. 2
- [32] Jiahao Liang, Huafeng Shi, and Weihong Deng. Exploring disentangled content information for face forgery detection. In *European Conference on Computer Vision*, pages 128–145. Springer, 2022. 3
- [33] Li Lin, Neeraj Gupta, Yue Zhang, Hainan Ren, Chun-Hao Liu, Feng Ding, Xin Wang, Xin Li, Luisa Verdoliva, and Shu Hu. Detecting multimedia generated by large ai models: A survey. *Arxiv Preprint Arxiv:2402.00045*, 2024. 3
- [34] Li Lin, Xinan He, Yan Ju, Xin Wang, Feng Ding, and Shu Hu. Preserving fairness generalization in deepfake detection. In *Proceedings of the IEEE/CVF Conference on Computer Vision and Pattern Recognition (CVPR)*, pages 16815–16825, 2024. 3
- [35] Zhengzhe Liu, Xiaojuan Qi, and Philip HS Torr. Global texture enhancement for fake face detection in the wild. In *Proceedings of the IEEE/CVF conference on computer vision and pattern recognition*, pages 8060–8069, 2020. 3
- [36] David Lopez-Paz and Marc’Aurelio Ranzato. Gradient episodic memory for continual learning. *Advances In Neural Information Processing Systems*, 30, 2017. 4
- [37] Peter Lorenz, Ricard L Durall, and Janis Keuper. Detecting images generated by deep diffusion models using their local intrinsic dimensionality. In *International Conference on Computer Vision*, pages 448–459, 2023. 3
- [38] Francesco Marra, Cristiano Saltori, Giulia Boato, and Luisa Verdoliva. Incremental learning for the detection and classification of gan-generated images. In *2019 IEEE international workshop on information forensics and security (WIFS)*, pages 1–6. IEEE, 2019. 3
- [39] Momina Masood, Mariam Nawaz, Khalid Mahmood Malik, Ali Javed, Aun Irtaza, and Hafiz Malik. Deepfakes generation and detection: State-of-the-art, open challenges, countermeasures, and way forward. *Appl. Intell.*, pages 1–53, 2022. 3
- [40] Aakash Varma Nadimpalli and Ajita Rattani. Gbdf: gender balanced deepfake dataset towards fair deepfake detection. *Arxiv Preprint Arxiv:2207.10246*, 2022. 3
- [41] Huy H Nguyen, Fuming Fang, Junichi Yamagishi, and Isao Echizen. Multi-task learning for detecting and segmenting manipulated facial images and videos. In *International Conference on Biometrics Theory, Applications and Systems*, pages 1–8. IEEE, 2019. 2
- [42] Alex Nichol, Prafulla Dhariwal, Aditya Ramesh, Pranav Shyam, Pamela Mishkin, Bob McGrew, Ilya Sutskever, and Mark Chen. Glide: Towards photorealistic image generation and editing with text-guided diffusion models. *Arxiv Preprint Arxiv:2112.10741*, 2021. 3
- [43] Kun Pan, Yifang Yin, Yao Wei, Feng Lin, Zhongjie Ba, Zhenguang Liu, Zhibo Wang, Lorenzo Cavallaro, and Kui Ren. Dfil: Deepfake incremental learning by exploiting domain-invariant forgery clues. In *Proceedings of the 31st ACM International Conference on Multimedia*, pages 8035–8046, 2023. 3
- [44] Wenbo Pu, Jing Hu, Xin Wang, Yuezun Li, Shu Hu, Bin Zhu, Rui Song, Qi Song, Xi Wu, and Siwei Lyu. Learning a deep dual-level network for robust deepfake detection. *Pattern Recogn.*, 130:108832, 2022. 3
- [45] Danfeng Qin, Chas Lechner, Manolis Delakis, Marco Fornoni, Shixin Luo, Fan Yang, Weijun Wang, Colby Banbury, Chengxi Ye, Berkin Akin, et al. Mobilenetv4: universal models for the mobile ecosystem. In *European Conference on Computer Vision*, pages 78–96. Springer, 2024. 4, 5, 6

- [46] Aditya Ramesh, Prafulla Dhariwal, Alex Nichol, Casey Chu, and Mark Chen. Hierarchical text-conditional image generation with clip latents. *Arxiv Preprint Arxiv:2204.06125*, 1(2):3, 2022. 3
- [47] Tal Ridnik, Emanuel Ben-Baruch, Asaf Noy, and Lih Zelnik-Manor. Imagenet-21k pretraining for the masses. *Arxiv Preprint Arxiv:2104.10972*, 2021. 6
- [48] David Rolnick, Arun Ahuja, Jonathan Schwarz, Timothy Lillicrap, and Gregory Wayne. Experience replay for continual learning. *Advances In Neural Information Processing Systems*, 32, 2019. 2, 5, 6
- [49] Robin Rombach, Andreas Blattmann, Dominik Lorenz, Patrick Esser, and Björn Ommer. High-resolution image synthesis with latent diffusion models. In *Proceedings of the IEEE/CVF Conference on Computer Vision and Pattern Recognition (CVPR)*, pages 10684–10695, 2022. 2
- [50] Andreas Rossler, Davide Cozzolino, Luisa Verdoliva, Christian Riess, Justus Thies, and Matthias Niessner. Faceforensics++: Learning to detect manipulated facial images. In *Proceedings of the IEEE/CVF International Conference on Computer Vision (ICCV)*, 2019. 2
- [51] Chitwan Saharia, William Chan, Saurabh Saxena, Lala Li, Jay Whang, Emily L Denton, Kamyar Ghasemipour, Raphael Gontijo Lopes, Burcu Karagol Ayan, Tim Salimans, et al. Photorealistic text-to-image diffusion models with deep language understanding. *Adv. Neur. In.*, 35:36479–36494, 2022. 3
- [52] Fahad Sarfraz, Elahe Arani, and Bahram Zonooz. Error sensitivity modulation based experience replay: Mitigating abrupt representation drift in continual learning. In *The Eleventh International Conference on Learning Representations*, 2023. 2, 5, 6
- [53] Francesco Tassone, Luca Maiano, and Irene Amerini. Continuous fake media detection: Adapting deepfake detectors to new generative techniques. *Comput. Vis. Image Und.*, 249: 104143, 2024. 1, 2, 3
- [54] Loc Trinh and Yan Liu. An examination of fairness of ai models for deepfake detection. *Ijcai*, 2021. 3
- [55] Shaheen Usmani, Sunil Kumar, and Debanjan Sadhya. Enhancing generalization ability in deepfake detection via continual learning. In *Proceedings of the Fifteenth Indian Conference on Computer Vision, Graphics and Image Processing (ICVGIP)*, 2024. 3
- [56] Guido M Van de Ven and Andreas S Tolias. Three scenarios for continual learning. *Arxiv Preprint Arxiv:1904.07734*, 2019. 2
- [57] Pavan Kumar Anasosalu Vasu, James Gabriel, Jeff Zhu, Oncel Tuzel, and Anurag Ranjan. Fastvit: A fast hybrid vision transformer using structural reparameterization. In *Proceedings of the IEEE/CVF international conference on computer vision*, pages 5785–5795, 2023. 4, 5, 6
- [58] Sheng-Yu Wang, Oliver Wang, Richard Zhang, Andrew Owens, and Alexei A Efros. Cnn-generated images are surprisingly easy to spot... for now. In *Conference on Computer Vision and Pattern Recognition*, pages 8695–8704, 2020. 3
- [59] Kyle Wiggers. Deepfake detectors and datasets exhibit racial and gender bias, usc study shows. In *VentureBeat*, <https://tinyurl.com/ms8zbu6f>, 2021. 3
- [60] Sanghyun Woo, Shoubhik Debnath, Ronghang Hu, Xinlei Chen, Zhuang Liu, In So Kweon, and Saining Xie. Convnext v2: Co-designing and scaling convnets with masked autoencoders. In *Proceedings of the IEEE/CVF conference on computer vision and pattern recognition*, pages 16133–16142, 2023. 4, 5, 6
- [61] Ying Xu, Philipp Terhörst, Kiran Raja, and Marius Pederesen. A comprehensive analysis of ai biases in deepfake detection with massively annotated databases. *Arxiv Preprint Arxiv:2208.05845*, 2022. 3
- [62] et al. Yan et al. Transcending forgery specificity with latent space augmentation for generalizable deepfake detection. In *Proceedings of the IEEE/CVF Conference on Computer Vision and Pattern Recognition (CVPR)*, 2024. Open Access version available on the CVF website. 3
- [63] Zhiyuan Yan, Yong Zhang, Yanbo Fan, and Baoyuan Wu. Ucf: Uncovering common features for generalizable deepfake detection. In *Proceedings of the IEEE/CVF International Conference on Computer Vision (ICCV)*, pages 22412–22423, 2023. 3
- [64] Zhiyuan Yan, Yandan Zhao, Shen Chen, Xinghe Fu, Taiping Yao, Shouhong Ding, and Li Yuan. Generalizing deepfake video detection with plug-and-play: Video-level blending and spatiotemporal adapter tuning. *Arxiv Preprint Arxiv:2408.17065*, 2024. 3
- [65] Shanmin Yang, Shu Hu, Bin Zhu, Ying Fu, Siwei Lyu, Xi Wu, and Xin Wang. Improving cross-dataset deepfake detection with deep information decomposition. *Arxiv Preprint Arxiv:2310.00359*, 2023. 3
- [66] Xin Yang, Yuezun Li, and Siwei Lyu. Exposing deep fakes using inconsistent head poses. In *International Conference on Acoustics, Speech and Signal Processing*, pages 8261–8265. IEEE, 2019. 2
- [67] Kelu Yao, Jin Wang, Boyu Diao, and Chao Li. Towards understanding the generalization of deepfake detectors from a game-theoretical view. In *2023 IEEE/CVF International Conference on Computer Vision (ICCV)*, pages 2031–2041, 2023. 3
- [68] Ke-Yue Zhang, Taiping Yao, Jian Zhang, Ying Tai, Shouhong Ding, Jilin Li, Feiyue Huang, Haichuan Song, and Lizhuang Ma. Face anti-spoofing via disentangled representation learning. In *Computer Vision—ECCV 2020: 16th European Conference, Glasgow, UK, August 23–28, 2020, Proceedings, Part XIX 16*, pages 641–657. Springer, 2020. 3
- [69] Lei Zhang, Hao Chen, Shu Hu, Bin Zhu, Xi Wu, Jinrong Hu, and Xin Wang. X-transfer: A transfer learning-based framework for robust gan-generated fake image detection. *Arxiv Preprint Arxiv:2310.04639*, 2023.
- [70] Peng Zheng, Hao Chen, Shu Hu, Bin Zhu, Jinrong Hu, Ching-Sheng Lin, Xi Wu, Siwei Lyu, Guo Huang, and Xin Wang. Few-shot learning for misinformation detection based on contrastive models. *Electronics*, 13(4):799, 2024. 3
- [71] Bojia Zi, Minghao Chang, Jingjing Chen, Xingjun Ma, and Yu-Gang Jiang. Wilddeepfake: A challenging real-world dataset for deepfake detection. In *Proceedings of the 28th ACM International Conference on Multimedia*, pages 2382–2390, 2020. 5